crystals

MDPI

Article

Bis (Diamines) Cu and Zn Complexes of Flurbiprofen as Potential Cholinesterase Inhibitors: In Vitro Studies and Docking Simulations

Muhammad Jamil [1,2], Nargis Sultana [2], Rizwan Ashraf [2], Maryam Bashir [2], Muhammad Fayyaz ur Rehman [2], Fariha Kanwal [3], Humna Ellahi [4], Changrui Lu [1,*], Wei Xing Zhang [5,*] and Muhammad Ilyas Tariq [2,*]

1 Department of Chemistry, Chemical Engineering and Biotechnology, Donghua University, Shanghai 201620, China; muhammadjameel026@gmail.com
2 Institute of Chemistry, University of Sargodha, Sargodha 40100, Pakistan; nargis.sultana@uos.edu.pk (N.S.); chemist_uos@hotmail.com (R.A.); maryambashir760@gmail.com (M.B.); muhammad.fayyaz@uos.edu.pk (M.F.u.R.)
3 Med-X Research Institute, School of Biomedical Engineering, Shanghai Jiao Tong University, Shanghai 200240, China; Fariha@sjtu.edu.cn
4 Department of Psychiatry, Lahore General Hospital, Lahore 54000, Pakistan; humnahammad@gmail.com
5 Department of Critical Care Medicine, Shanghai General Hospital, School of Medicine, Shanghai Jiao Tong University, Shanghai 200240, China
* Correspondence: crlu@dhu.edu.cn (C.L.); weixing.zhang@shgh.cn (W.X.Z.); tariqmi2000@yahoo.com (M.I.T.)

Citation: Jamil, M.; Sultana, N.; Ashraf, R.; Bashir, M.; Rehman, M.F.u.; Kanwal, F.; Ellahi, H.; Lu, C.; Zhang, W.X.; Tariq, M.I. Bis (Diamines) Cu and Zn Complexes of Flurbiprofen as Potential Cholinesterase Inhibitors: In Vitro Studies and Docking Simulations. *Crystals* **2021**, *11*, 208. https://doi.org/10.3390/cryst11020208

Academic Editor: Ana Garcia-Deibe

Received: 27 January 2021
Accepted: 14 February 2021
Published: 20 February 2021

Abstract: Alzheimer's disease (AD) causes dementia and continuous damage to brain cells. Cholinesterase inhibitors can alleviate the condition by increasing communication between the nerve cells and reducing the risk of dementia. In an effort to treat Alzheimer's disease, we synthesized flurbiprofen-based diamines (1,2 diaminoethane and 1,3 diaminopropane) Zn(II), Cu(II) metal complexes and characterized them by single-crystal X-ray analysis, NMR, (FT)-IR, UV-Vis, magnetic susceptibility, elemental analysis and conductivities measurements. Synthesized diamine metal complexes appeared in ionic forms and have distorted octahedral geometry based on conductivity studies, magnetic susceptibility and electronic studies. Single crystal X-ray diffraction analysis confirmed (2b) $Cu(H_2O)_2(L1)_2(L2)_2$ complex formation. Moreover, we tested all synthesized metal complexes against the cholinesterase enzyme that showed higher inhibition potential. In general, copper metal complexes showed higher inhibitory activities than simple metal complexes with flurbiprofen. These synthesized metal complexes may derive more effective and safe inhibitors for cholinesterases.

Keywords: Alzheimer's disease; diamines; flurbiprofen; cholinesterases; metal complexes

1. Introduction

Around the globe, 2.5 to 4.0 million elderly people suffer from Alzheimer's disease (AD), manifested by long-term neurodegeneration, loss of neural functions and cognitive abilities that ultimately lead to death [1]. Studies show that numerous disorders, including AD, correlate with high cholinesterase activity. Cholinesterase belongs to the serine hydrolases family, consisting of acetylcholinesterase (AChE) and butyryl-cholinesterase (BChE) [2,3]. Many physiological processes have been controlled by cholinesterase in either a direct or indirect way. Cholesterol overexpression may lead to numerous disorders like ataxia, myasthenia gravis and Parkinson's disease [4,5]. To combat and treat these disorders, researchers have been looking for synthetic and natural inhibitors of cholinesterase. Physostigmine existed as the first cholinesterase inhibitor (ChEI) explored for the cure of AD [6]. Tacrine was the first approved drug for treating AD. Donepezil was permitted in 1996 for the treatment of mild-to-moderate AD. All these compounds, rivastigmine, galantamine, metrifonate, phenserine, physostigmine and tacrine, showed effective inhibition of human AChE and BuChE [7–13]. To target neuroinflammation and vesicant-induced

inflammation, studies have focused on NSAID-AChEI complexes [14–17]. Current "second-generation" AChEIs also demonstrate some side effects such as diarrhoea, nausea, anorexia and vomiting [18]. So far, no proper treatment exists for these neurodegenerative disorders like Alzheimer's disease; hence, researchers have been avidly seeking a proper cure for these neurodegenerative problems.

Currently, several potent inhibitors for cholinesterase exist in the market as first-line treatment for these neurodegenerative problems. However, effective treatment requires more effective inhibitors with safe and extraordinary potential for cholinesterase control, which demands further exploration of anticholinesterase compounds. Recently, organic metal complexes have shown positive effects on these neurodegenerative disorders [19]. For example, Pt(II) complexes with 1,10-phenanthroline ligands can inhibit cholinesterase and reduce Aβ aggregation and Aβ-induced synaptotoxicity [20]. Similarly, previous studies have prepared and analyzed metal complexes of bis (thiosemicarbazone) for cholinesterase inhibition along with a reduction in levels of Aβ aggregations [21].

Some studies showed that Cu or Zn complexes with 8-hydroxyquinoline ligands could induce metal-dependent metalloprotease activity, which degrades Aβ aggregations and ultimately reduces the risk of AD [22–24]. Mono-, bis- and tris-diamine conjugated ligands have been found more water-soluble with an enhanced H-bonding network. By using this property, various ligand-metal complexes have been designed with anti-cancer properties [25–28]. Flurbiprofen-tacrine conjugates and tris-diamine conjugates of flurbiprofen have been reported as cholinesterase inhibitors, where flurbiprofen backbone was found to augment the inhibitory activity [17,29]. Here, we present synthesis and characterization of a relatively new class of flurbiprofen (a propionic acid carboxylate) and its transition metal complexes with diamines (1,2-diaminoethane and 1,3-diaminopropane) as effective cholinesterase inhibitors.

2. Materials and Methods

Analytical grade reagents and chemicals including metal salts (copper acetate, zinc acetate), 1,2-diaminoethane, 1,3-diaminopropane, flurbiprofen acid and solvents were purchased from Merck Millipore and Sigma Aldrich, England. Reagent for cholinesterase assay including electric eel acetyl cholinesterase (AChE), equine serum autyrylcholinesterase (BChE), 5,5-dithio-bis-(2-nitrobenzoic acid), acetylthiocholine iodide (ATChI), butyryl thiocholine Iodide (BChI), galantamine hydrobromide and donepezil were obtained from Sigma Aldrich, England, while a μQuant microplate spectrophotometer (MQX200, BioTek, Winooski, VT, USA) was used for assay monitoring. Aluminum-backed TLC plates were used to analyse the products. UV/visible, infrared spectra and ^{1}H-/^{13}C-NMR spectra were obtained using Jenway 6505 (Keison Products, Chelmsford, UK), Shimadzu (FT)IR-8400S (Shimadzu Scientific Instruments Inc. Kyoto, Japan), and Bruker AM 300/400 (Bruker's AVANCE Tech, Billerica, MA, USA) spectrometers, respectively, as described in [30]. Stanton SM12/S Gouy's balance was used to to determine magnetic susceptibility. The Elemental Analyzer (Perkin Elmer, USA) and Inolab Conductivity Bridge 720 were used to determine the percentage of C, H, N, M and molar conductance.

2.1. Synthesis of Flurbiprofen Metal Complexes (1a-b)

The potassium salt of flurbiprofen (FLP-K) was prepared by adding 20 mL of 0.01 mol flurbiprofen acid (2.44 g) solution in de-ionized water to 0.01 mol KOH (0.56 g). A dropwise addition of 0.005 mol metal acetate solution (10 mL) to the FLP-K solution with continuous stirring for 20 min in a round bottom flask at room temperature resulted in the formation of the metal-flurbiprofen complex (1a-b) with the characteristic colored precipitates. The precipitates were filtered, followed by subsequent washings with de-ionized water and ethanol. After washing, precipitates were dried at the room temperature.

2.1.1. $Zn(H_2O)_2(L)_2$ (1a)

$C_{30}H_{28}F_2O_6Zn$ (1a) was synthesized by the method given in Section 2.1 using 0.005 moles zinc acetate (0.971 g). A white solid product with 83%, yield was obtained showing a melting point of 183 °C. Analytical calculations for $C_{30}H_{28}F_2O_6Zn$ (%) was found to be: C, 61.29; H, 4.80, found: C, 61.22; H, 4.82. Selected FT-IR data (KBr, cm^{-1}) show: $\overline{v}(M{\leftarrow}H_2O)$ 3653 cm^{-1}, $\overline{v}(M{\leftarrow}O)$ 484 cm^{-1}, $\overline{v}$ (CO)1650–1730 cm^{-1}, $\overline{v}$ (Ar C = C)1500–1590 cm^{-1}, $\overline{v}$(C-H) 2700–2900 cm^{-1} and disappearance of the broad $\overline{v}$ (OH) peak at 3200–3400, λ_{max} (cm^{-1}) = 29543, $\Omega^{-1}cm^2mol^{-1}$ = 18, μeff = diamagnetic, ^{1}H NMR (400.13 MHz, [d_6]DMSO, 25 °C): δ = 6.64 (d, ^3J = 8 Hz, 4H, H-9, H-13, H-9′, H-13′), 6.58 (t, ^3J = 7 Hz, 4H, H-10, H-12, H-10′, H-12′), 6.55–6.51 (m, 4H, H-5, H-11, H-5′, H-11′), 6.36 (d, ^3J = 8 Hz, 2H, H-4, H-4′), 6.33 (s, 2H, H-8, H-8′), 2.78–2.71 (m, 2H, H-2, H-2′), 0.49 (d, ^3J = 8 Hz, 6H, H-1, H-1′) ppm. ^{13}C NMR (100.61 MHz, [d_6] DMSO, 25 °C): δ = 178.7, 160.0, 157.6, 135.2, 130, 128.7, 128.6, 127.6, 125.8, 124.2, 115.1, 45.8, 19.7.

2.1.2. $Cu(H_2O)_2(L)_2$ (1b)

Copper acetate 0.908 g (0.005 moles) was used to synthesize $Cu(H_2O)_2(C_{15}H_{12}FO_2)_2$ (1b) using the method given in Section 2.1. A light green solid product with a yield of 76% was obtained showing a melting point of 174–176 °C. Analytical calculations show (%): C, 61.48; H, 4.82, found: C, 61.44; H, 4.82. Selected FT-IR data (KBr, cm^{-1}): $\overline{v}(M{\leftarrow}H_2O)$ 3690 cm^{-1}, $\overline{v}(M{\leftarrow}O)$ 453 cm^{-1}, $\overline{v}$ (CO)1650–1730 cm^{-1}, $\overline{v}$ (Ar C = C)1500–1590 cm^{-1}, $\overline{v}$(C-H) 2700–2900 cm^{-1} and disappearance of the broad $\overline{v}$(OH) peak near 3200–3400, λ_{max} (cm^{-1}) = 15,219–15,412, $\Omega^{-1}cm^2mol^{-1}$ = 21, μeff = 1.7.

2.2. Synthesis of Bis (1,2-diaminoethane) Metal Flurbiprofen Complexes (2a-b)

Diaminoethane and flurbiprofen-metal complex conjugates were obtained by adding 1.42 mL of 0.02 moles 1,2-diaminoethane in flurbiprofen-metal complex (1a-b) solutions in 10 mL of ethanol/water (1:1). The mixture was stirred at room temperature for 25 min to obtain a clear blue solution. Crystals for diaminoethane and flurbiprofen-metal complexes were obtained by slow evaporation (2a-b).

2.2.1. $Zn(H_2O)_2$ $(C_2H_8N_2)_2$ $(C_{15}H_{12}FO_2)_2$ (2a)

A white solid product, $C_{34}H_{44}F_2N_4O_6Zn$ (2a), with a yield of 88% was obtained using the method given in Section 2.2. The melting point was found to be 222–224 °C. Analytical calculations for $C_{34}H_{44}F_2N_4O_6Zn$ (%): C, 57.67; H, 6.26; N, 7.91, found: C, 57.60; H, 6.29; N, 7.90. Selected FT-IR data (KBr, cm^{-1}): $\overline{v}(M{\leftarrow}H_2O)$ 3623 cm^{-1}, $\overline{v}(M{\leftarrow}N)$ 509 cm^{-1}, $\overline{v}$ (CO)1650–1730 cm^{-1}, $\overline{v}$(Ar C=C)1500–1590 cm^{-1}, $\overline{v}$(CH) 2700–2900 cm^{-1} and disappearance of the broad $\overline{v}$(OH) peak at 3200–3400 and $\overline{v}(M{\leftarrow}O)$peak, λ_{max} (cm^{-1}) = 30,816, Ω^{-1} cm^2mol^{-1} = 164, μeff = diamagnetic, ^{1}H NMR (400.13 MHz, [d_6]DMSO, 25 °C): δ = 7.51 (d, ^3J = 8 Hz, 4H, Ar*H*), 7.45 (t, ^3J = 7 Hz, 4H, Ar*H*), 7.40–7.35 (m, 4H, Ar*H*), 7.21–7.17 (m, 4H, Ar*H*), 3.59–3.53 (m, 2H, 2 × CH), 3.24–3.19 (m, 8H, 4×NH_2), 3.12–3.09 (m, 8H, 4×CH_2), 1.35 (d, ^3J = 8 Hz, 6H, 2×CH_3) ppm. ^{13}C NMR (100.61 MHz, [d_6] DMSO, 25 °C): δ = 177.8, 159.6, 157.3, 135.0, 129.9, 128.4, 128.2, 127.4, 125.2, 124.1, 114.9, 46.7, 46.2, 19.6.

2.2.2. $Cu(H_2O)_2$ $(L1)_2$ $(L)_2$ (2b)

$C_{34}H_{44}F_2N_4O_6Cu$ (2b) was synthesized as mentioned in Section 2.2 using 1.42 mL 1,2-diaminoethane (0.02 moles). Blue crystals with a yield of 84(%) were obtained. A melting point of 215–217 °C was observed. Analytical calculations for $C_{34}H_{44}F_2N_4O_6Cu$ (%): C, 57.82; H, 6.28; N, 7.93, found: C, 57.79; H, 6.24; N, 7.95. Selected FT-IR data (KBr, cm^{-1}): $\overline{v}(M{\leftarrow}H_2O)$ 3598 cm^{-1}, $\overline{v}(M{\leftarrow}N)$ 516 cm^{-1}, $\overline{v}$ (CO)1650–1730 cm^{-1}, $\overline{v}$(Ar C = C)1500–1590 cm^{-1}, $\overline{v}$(CH) 2700–2900 cm^{-1} and disappearance of the broad $\overline{v}$(O-H) peak at 3200–3400 and $\overline{v}(M{\leftarrow}O)$ peak, λ_{max} (cm^{-1}) = 16,749–16,810, $\Omega^{-1}cm^2mol^{-1}$ = 158, μeff = 1.9.

2.3. Synthesis of Bis (1,3-diaminopropane) Metal Flurbiprofen Complexes (3a-b)

To the ethanol/water (1:1) solution (10 mL) of flurbiprofen metal complexes (1a-b), 1.68 mL of 1,3-diaminopropane (0.02 mol) was added to obtain 1,3-diaminopropane diamines and flurbiprofen mixed ligand complexes. After 25 min stirring at room temperature, a clear blue solution was obtained that crystalized upon slow evaporation to give bis (1,3-diaminopropane) metal flurbiprofen complex crystals (3a-b).

2.3.1. $Zn(H_2O)_2$ $(L1)_2$ $(L)_2$ (3a)

A white solid product, $C_{36}H_{48}F_2N_4O_6Zn$ (3a), with a yield of 80%, was synthesized using the method mentioned in Section 2.3. The melting point was observed as 218–220 °C. Analytical calculations show (%): C, 58.73; H, 6.57; N, 7.61, found: C, 57.64; H, 6.55; N, 7.96. Selected FT-IR data (KBr, cm^{-1}): $\overline{v}(M{\leftarrow}H_2O)$ 3623 cm^{-1}, $\overline{v}(M{\leftarrow}N)$ 509 cm^{-1}, $\overline{v}$ (CO)1650–1730 cm^{-1}, $\overline{v}$(Ar C = C)1500–1590 cm^{-1}, $\overline{v}$(CH) 2700–2900 cm^{-1} and disappearance of broad $\overline{v}$(O-H) at 3200–3400 cm^{-1} and $\overline{v}(M{\leftarrow}O)$ peak, λ_{max} (cm^{-1}) = 20,842, ε cm^2mol^{-1} = 160, μeff = diamagnetic, ^{1}H NMR (400.13 MHz, [d_6]DMSO, 25 °C): δ = 7.50 (d, ^3J = 8 Hz, 4H, Ar*H*), 7.45 (t, ^3J = 7 Hz, 4H, Ar*H*), 7.40–7.35 (m, 4H, Ar*H*), 7.22 (d, ^3J = 8 Hz, 2H, Ar*H*), 7.20 (s, 2H, Ar*H*), 3.59–3.53 (m, 2H, 2 × CH), 3.47–3.42 (m, 8H, 4×NH_2), 2.68–2.64 (m, 8H, 4×CH_2), 2.01–1.95 (m, 4H, 2×CH_2), 1.35 (d, ^3J = 8 Hz, 6H, 2×CH_3) ppm. ^{13}C NMR (100.61 MHz, [d_6] DMSO, 25 °C): δ = 177.8, 159.6, 157.3, 135.0, 129.9, 128.4, 128.2, 127.4, 125.2, 124.1, 114.9, 46.2, 39.2, 38.6, 19.6.

2.3.2. $Cu(H_2O)_2$ $(L1)_2$ $(C_L)_2$ (3b)

The general method given in Section 2.3 was used to obtain the compound $C_{36}H_{48}F_2N_4O_6Zn$ (3b) with a yield of 80(%); melting point of 210–212 °C; analytical calculations (%) of C, 58.88; H, 6.59; N, 7.63, found: C, 58.80; H, 6.49; N, 7.79. Selected FT-IR data (KBr, cm^{-1}): $\overline{v}(M{\leftarrow}H_2O)$ 3598 cm^{-1}, $\overline{v}(M{\leftarrow}N)$ 516 cm^{-1}, $\overline{v}$ (CO)1650–1730 cm^{-1}, $\overline{v}$(Ar C = C)1500–1590 cm^{-1}, $\overline{v}$(CH) 2700–2900 cm^{-1} and disappearance $\overline{v}(M{\leftarrow}O)$ peak and broad $\overline{v}$(O-H) peak at 3200–3400 cm^{-1}, λ_{max} (cm^{-1}) = 16,735–16,788, $\Omega^{-1}cm^2mol^{-1}$ = 150, μeff = 1.9.

2.4. Molecular Docking Simulations

The Three-dimensional structures of human AChE and BChE were obtained from the Protein Data Bank (PDB) with PDB IDs of 4EY4 (X-ray structure with 2.15 Å resolution) and 6ESY (X-ray structure with 2.80 Å resolution), respectively, and attached ligands/water molecules were removed. The Cu-bisdiamine-flurbiprofen complex, 2b (C34H44F2N4O6Cu), was docked against the human AChE and BChE enzymes to map the protein–ligand interactions and binding energies. Cu-bisdiamines and flurbiprofen were also docked individually to calculate the efficacy of 2b. The crystal structure of 2b was used in the docking where the AMBER03 force field and a modified AutoDock-LGA algorithm module were used in YASARA software [31] to perform molecular docking simulations. Binding energies and dissociation constants were obtained by running the 100 simulations for each ligand, where the seed value was set to 1000 [32]. Protein–ligand interactions were extracted and mapped using PyMol (The PyMOL Molecular Graphics System, Version 2.0 Schrödinger, LLC. New York, NY, USA) and LigPlus http://www.ebi.ac.uk/thornton-srv/software/LIGPLOT/).

2.5. Determination of AChE and BChE Inhibitory Activity

A modified Ellman's method [33] was used to determine the AChE and BChE inhibitory activity of metal complexes [34]. Phosphate buffer (0.1 M KH_2PO_4/K_2HPO_4, pH 8.0) was used to prepare metal complex samples, enzymes and standard solutions. 0.03 U/mL of AChE and BChE were added to a 10 μL metal complex solution (0–50 μM), and the mixture was incubated for 10 min at room temperature. Then, 25 μL of 1 mM of either ATChI or BTChI was added, and the sample mixture was incubated for the next 15 min followed by the addition of 25 μL of 3 mM DTNB before taking absorbance at

412 nm using a μQuant microplate spectrophotometer. Microwells with DTNB were used as blank. All reactions were made in triplicate, and the IC50 values were calculated for each sample. Galantamine and donepezil are well-known cholinesterase inhibitors and were used as reference drugs.

3. Results

3.1. Synthesis

In this study, we synthesized transition metal complexes of flurbiprofen with propanediamine (1,3-diaminopropane) and ethylene-diamine (1,2-diaminoethane). Next, we evaluated these metal complexes using magnetic susceptibility, elemental analysis and FT-IR, UV-VIS spectroscopy, conductivity measurements and X-ray analysis, ^{1}H-NMR, ^{13}C-NMR. These metal complexes are ionic based on conductivity rearmaments and have distorted octahedral geometry based on electronic studies and magnetic susceptibility studies. Synthesis of these metal complexes caused little to no pollution (green synthesis) because we used harmless solvents like water and ethanol. These metal complexes can only be obtained in water, but for precise crystals, ethanol was also used. Figure 1 illustrates the scheme of synthesis for these metal complexes.

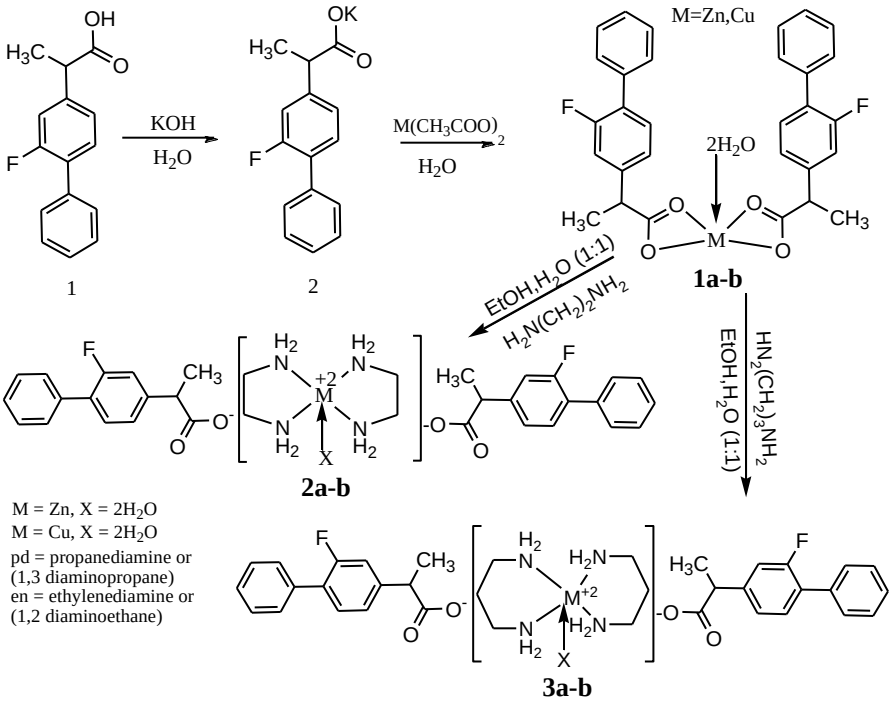

Figure 1. Scheme for the synthesis of bis (1,2-diaminoethan and 1,3-diaminoprpane) metal flurbiprofen complexes. (Flurbiprofen ($C_{15}H_{12}FO_2$) = L, 1,2-diaminoethane ($C_2H_8N_2$) = L1, 1,3-diaminpropane ($C_3H_{10}N_2$) = L2.).

3.2. X-ray Crystallography

Among all the simple and bis (1,2-diaminoethan and 1,3-diaminoprpane)-derived metal complexes of flurbiprofen, only $Cu(H_2O)_2(L1)_2$ $(L)_2$ (2b) yielded blue crystals which were suitable for X-ray analysis. The coordination sphere appears octahedral with a basal plane A (N1/N2/N1^{i}/N2^{i} i = 1 − x, − y, 1 − z) around the copper cation in (2b) with two apical O-atoms from two water and four nitrogen atoms from two 1,2-diaminoethane. In the equatorial plane, the copper atom appears in the centre. The Cu-N bonds fall within the experimental error [1.998(4)-2.011(4) Å], and the Cu-O bond is 2.605(5) Å. Two symmetry operations relate flurbiprofen anions. In the flurbiprofen anion, the terminal benzene ring (C10-C15) is planar with r.m.s deviations of 0.0032, 0.0084 and 0.0023 Å with acetyl moiety (O1/O2/C1/C2) and the fluorophenyl ring (C4-C9/F1).

The crystal contains an infinite polymeric network due to hydrogen bonding of N-H···O, O-H···O and C-H···F with two-dimensional crystallographic base vectors [100], [1] in the plane (0 1 0). The ORTEP diagram of 2b with a 50% probability level and the two-dimensional polymeric network are displayed in Figure 2.

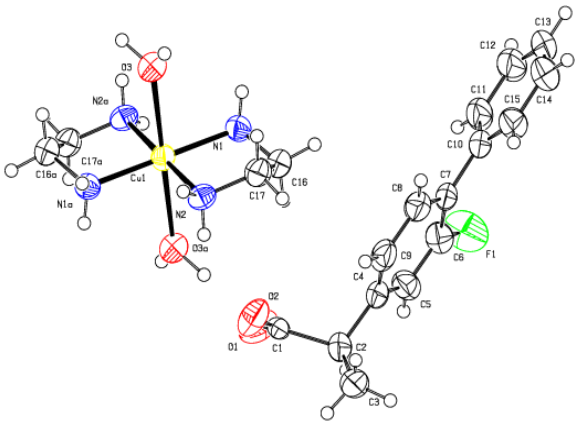

(**a**)

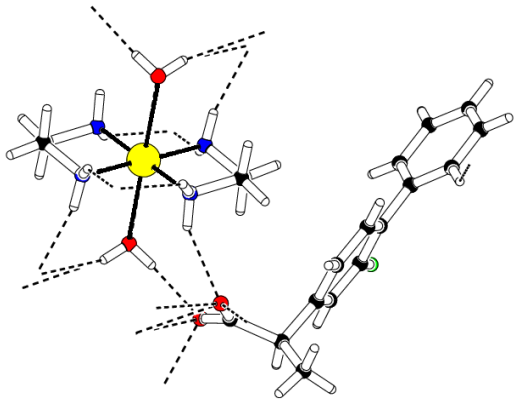

(**b**)

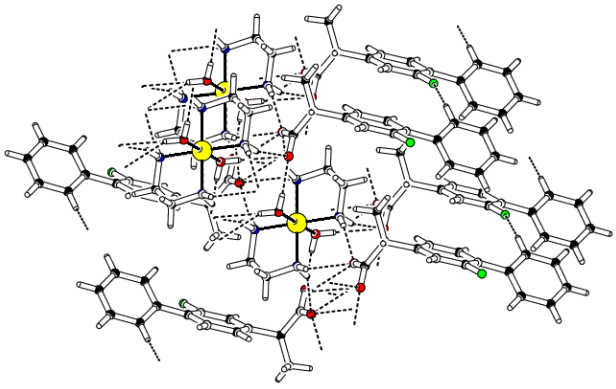

(**c**)

Figure 2. ORTEP diagram of 2b with thermal ellipsoids drawn at 50% probability level. The H-atoms are shown as small circles of arbitrary radii. Symmetry code i = 1 − x, − y, 1 − z (**a**,**b**). The two-dimensional polymeric network due to various H-bonding of 2b (**c**) (CCDC# 1965852).

3.3. NMR Analysis

Next, we characterize zinc complexes of flurbiprofen by ^{1}H NMR and ^{13}C NMR in d_6DMSO. The ^{1}H NMR of zinc complex of flurbiprofen (1a) indicates the complex formation. Singlet, duplet and multiplet with chemical shift values of 6.64, 6.58, 6.55–6.51, 6.36 and 6.33 ppm indicate aromatic protons. A shielded signal for the methyl group at 0.49 ppm is observed, and a multiplet near 2.78–2.71 ppm reflects tertiary carbon attached to the aromatic ring. A characteristic downfield signal in ^{13}C-NMR at 178.5 ppm indicates that aromatic carbon is directly attached with a tertiary carbon. Up-field signals at 160.0, 157.6, 135.2, 130.2, 128.7, 128.6, 127.6, 125.8, 124.2 ppm show other aromatic carbons. A chemical shift value at 45.8 ppm indicates a tertiary carbon.

The zinc flurbiprofen complex (2a) complex was synthesized showing the ^{1}H NMR peak shifting at 7.51, 7.45, 7.40–7.35, 7.21–7.17 ppm for aromatic protons and multiplet (3.59–3.53) ppm for hydrogen of tertiary methyl groups shift downfield. This indicates a decrease in (M-O) interaction and an increase in (M-N) interaction, which reflects the formation of (2a).

Chemical shifts at 3.12–3.09 ppm ($4\times CH_2$) and 3.24–3.19 ppm ($4\times NH_2$) confirm the synthesis of (2a). Two new peaks at 46.7 ppm ($2\times CH_2$) and 46.2 ppm ($2\times CH_2$) in ^{13}C NMR of (2a) indicate that $4\times CH_2$ of 1,2-diaminoethane are interacting with zinc metal, which suggest a synthesis of (2a). Similarly, for the synthesis of bis (1,3-diaminopropane) zinc flurbiprofen complex (3a), 1,3-diaminopropane was added to (1a). The ^{1}H NMR and ^{13}C NMR chemical shifts values of ^{1}H NMR at (7.50, 7.45, 7.40–7.35, 7.22, 7.20 ppm) for aromatic protons and multiplet (3.59–3.53) ppm for tertiary methyl groups shift towards the downfield region. New signals of multiplet at 3.47–3.42 ppm ($4\times NH_2$), 2.68–2.64 ppm ($4\times CH_2$) and 2.01–1.95 ppm ($2\times CH_2$) confirm the formation of (3a). The ^{13}C NMR of (3a) shows three new peaks at 46.2 ppm ($2\times CH_2$), 39.2 ppm ($2\times CH_2$) and 38.6 ppm ($2\times CH_2$), indicating the ($6\times CH_2$) of (1,3-diaminopropane) are interacting with zinc metal, which suggests a synthesis of (3a).

3.4. FT-IR Analysis

We also performed an FT-IR analysis of metal complexes for the structural confirmation of metal complexes. IR peaks near 1419–1476 cm^{-1} suggest that these peaks belong to (aromatic–CH) functional groups. The peaks appearing near the 461–479 cm^{-1} range reflect (M←O) metal–oxygen bonds formation and peaks near 523–572 cm^{-1} show the formation of (M←N) metal–nitrogen bonds. IR analysis of the complexes does not show the (M-N) metal–nitrogen peaks for (1a-b) due to synthesis from transition metals and flurbiprofen acid. However, if the addition of (1,3-diaminopropane) and (1,2-diaminoethane) to simple flurbiprofen complexes (1a-b) leads to the formation of (2a-b) and (3a-b), the (M-N) metal peaks appear near 514–580 cm^{-1}, suggesting the formation of a metal–ligand chelating bond between the nitrogen of 1,2-diaminoethane and 1,3-diaminopropane and metal.

3.5. UV/vis and Magnetic Susceptibility

In addition to other spectroscopic techniques, UV-visible analysis was performed to support the complex formation and confirm the symmetry of metal complexes. The symmetry of transition metal complexes was deduced from several peaks observed. For each metal complex, the electronic spectra of 3d-transition metals were recorded in 10^{-3} to 10^{-5} M solutions in the range of 200–800 nm in DMSO. Only one peak at 29,543 cm^{-1} in Zn(II) complexes appears for (1a), 30,816 cm^{-1} in (2a) and 30,842 cm^{-1} in (3a), for metal to ligand charge transfer. The B.M. values were recorded as zero, suggesting the diamagnetic nature of these complexes. Only a single low-intensity broadband in the range of 15,219–15,412 cm^{-1} was observed for Cu(II) complexes for (1b), 16,749–16,810 cm^{-1} for (2b) and 16,735–16,788 cm^{-1} in (3b). The spectrum of these metal complexes indicates that the $^{2}E_g \rightarrow {}^{2}T_{2g}$ transition leads to distorted octahedral geometry of the metal complexes. The difference in the position of peaks is due to the difference in the size of ligands in (1b), (2b) and (3b) for copper complexes. Because different ligands possess different splitting in

d-orbitals of metal, B.M. values for copper complexes are measured near 1.7, 1.9 and 1.9, which suggests distorted octahedral geometry of copper complexes.

3.6. Elemental Analysis

Percentage analysis of C, H, N and all synthesized transition metal (II) complexes of flurbiprofen agreed with the calculated percentage values of their suggested molecular structures (Supplementary Materials). Both values fall under acceptable ranges (±0.03–0.95), which confirms the formation of suggested diamine-based transition metal (II) complexes.

3.7. Conductivity Measurements

Synthesized metal complexes were subjected to molar conductivities at room temperature. Conductivity measurements were performed to check the ionic and non-ionic nature of the metal complexes. All the metal complex solutions were prepared with a molar concentration of (1×10^{-3} M). Molar conductivities of synthesized flurbiprofen metal complexes (1a-b) measure 18 and 21 $\Omega^{-1}cm^2mol^{-1}$, indicating their non-ionic nature. However, as ethylene-diamine (1,2-diaminoethane) and propane-diamine (1,3-diaminopropane) were added to (1a-b) for the formation of bis (1,2-diaminoethane) metal flurbiprofen complexes (2a-b) and bis (1,3-diaminopropane) metal flurbiprofen complexes (3a-b), the conductance increased one order of magnitude to 164 and 158 $\Omega^{-1}cm^2mol^{-1}$ for (2a-b) and 160 and 150 $\Omega^{-1}cm^2mol^{-1}$ for (3a-b). This increase in conductivity of these bis (1,3-diaminopropane and 1,3-diaminopropane) flurbiprofen transition metal complexes indicates their electrolytic or ionic character.

3.8. Anticholinesterase Activity

Anti-cholinesterase activities of transition metal complexes of diamines (1,2-diaminoethane, 1,3-diaminopropane) with flurbiprofen (1a-b, 2a-b and 3a-b) are shown in Table 1. We observed that metal complexes of flurbiprofen derived from 1,2-diaminoethane (2a-b) show most potency as a cholinesterase inhibitor, with the lowest IC50 values compare to other series (1a-b and 3a-b). In general, the trend in cholinesterase inhibition follows the order 2a-b >3a-b >1a-b. This sequence indicates that nitrogen-containing transition metal complexes possess more cholinesterase inhibitory potency as compared to simple transition metal complexes. Table 2 shows the inhibitory activities of diamine-based metal in vitro.

Moreover, copper complexes exhibit higher activity and have the lowest IC50 values in our study. Among all the metal complexes, $Cu(H_2O)_2$ $(L1)_2$ $(L)_2$ (2b) showed inhibitory activities against AChE and BChE, with the lowest IC50 values, 3.0 ± 0.24 and 12.3 ± 0.21.

Table 1. Crystal data and structure refinement for 2b.

Identification Code	Shelx
Empirical formula	C34 H44 Cu F2 N4 O6
Formula weight	706.27
Temperature	296(2) K
Wavelength	0.71073 Å
Crystal system	Monoclinic
Space group	P 21/n
Unit cell dimensions	
a = 6.6291(8) Å	α = 90°
b = 40.392(5) Å	β = 112.243(6)°
c = 6.8061(9) Å	γ = 90°
Volume	1686.8(4) $Å^3$
Z	2

Table 1. *Cont.*

Identification Code	Shelx
Density (calculated)	1.391 Mg/m^3
Absorption coefficient	0.708 mm^{-1}
F(000)	742
Crystal size	0.420 × 0.280 × 0.200 mm^3
Theta range for data collection	1.008 to 27.356°.
Index ranges	$-8 \leq h \leq 7$, $-51 \leq k \leq 49$, $-5 \leq l \leq 8$
Reflections collected	10,124
Independent reflections	3611 [R(int) = 0.0400]
Completeness to theta = 25.242°	98.4%
Refinement method	Full-matrix least-squares on F^2
Data/restraints/parameters	3611/0/221
Goodness-of-fit on F^2	1.172
Final R indices [I > 2sigma(I)]	R1 = 0.0884, wR2 = 0.2301
R indices (all data)	R1 = 0.1181, wR2 = 0.2532
Extinction coefficient	n/a
Largest diff. peak and hole	1.684 and −0.713 e.$Å^{-3}$

Table 2. In vitro AChE and BChE inhibitory activities of compounds.

(1a-b, 2a-b and 3a-b)				
Sample Code	**Compounds**	**Anticholinesterase Activity * (IC_{50} μM)**		
		eeAChE	**eqBChE**	**SI**
1a	$Zn(H_2O)_2(L)_2$	32.3 ± 1.4	43.2 ± 1.23	1.3
2a	$Zn(H_2O)_2(L1)_2(L)_2$	3.5 ± 0.14	13.6 ± 0.38	5.4
3a	$Zn(H_2O)_2(L2)_2(L)_2$	9.3 ± 0.22	21.3 ± 2.31	2.2
1b	$Cu(H_2O)_2(L)_2$	22.5 ± 0.62	45.4 ± 1.45	2.0
2b	$Cu(H_2O)_2(L1)_2(L)_2$	3.0 ± 0.24	12.3 ± 0.21	4.1
3b	$Cu(H_2O)_2(L2)_2(L)_2$	3.4 ± 0.17	14.5 ± 0.27	4.2
A *	**Galantamine**	4.0 ± 0.10	15.0 ± 0.67	3.7
L	**Flurbiprofen**	45 ± 0.13	443 ± 30.73	9.5

* Experiments were performed thrice at 0.5 mM substrates.

3.9. Molecular Docking Studies

Molecular docking results are in agreement with in vitro choline esterase activities for the metal complex $Cu(H_2O)_2$ $(C_2H_8N_2)_2$ $(C_{15}H_{12}FO_2)_2$. FLP docking with *h*AChE shows π–π stacking with Trp^{86} and Tyr^{124}, while Tyr^{337} forms a hydrogen bond (Figure 3a). These interactions look similar to donepezil binding to the PAS (Peripheral Anionic Site), but interestingly Trp^{286} does not seem to be involved in FLP binding. Tyr337 is considered an entry point for the CAS (Catalytic Binding Site) [35,36] and it seems here FLP-Tyr^{337} interactions hinder the FLP entry deep into the CAS. The bis-diamine metal complex was found to interact with Glu^{81}, Trp^{86} and Asp^{131}. Bound water molecules were found to interact with Glu^{81} and Trp^{86}. Met^{85} interacts with metal ion, while one of the amines from each bis-diamine complex forms H-bonds with Asp^{131} (Figure 3b).

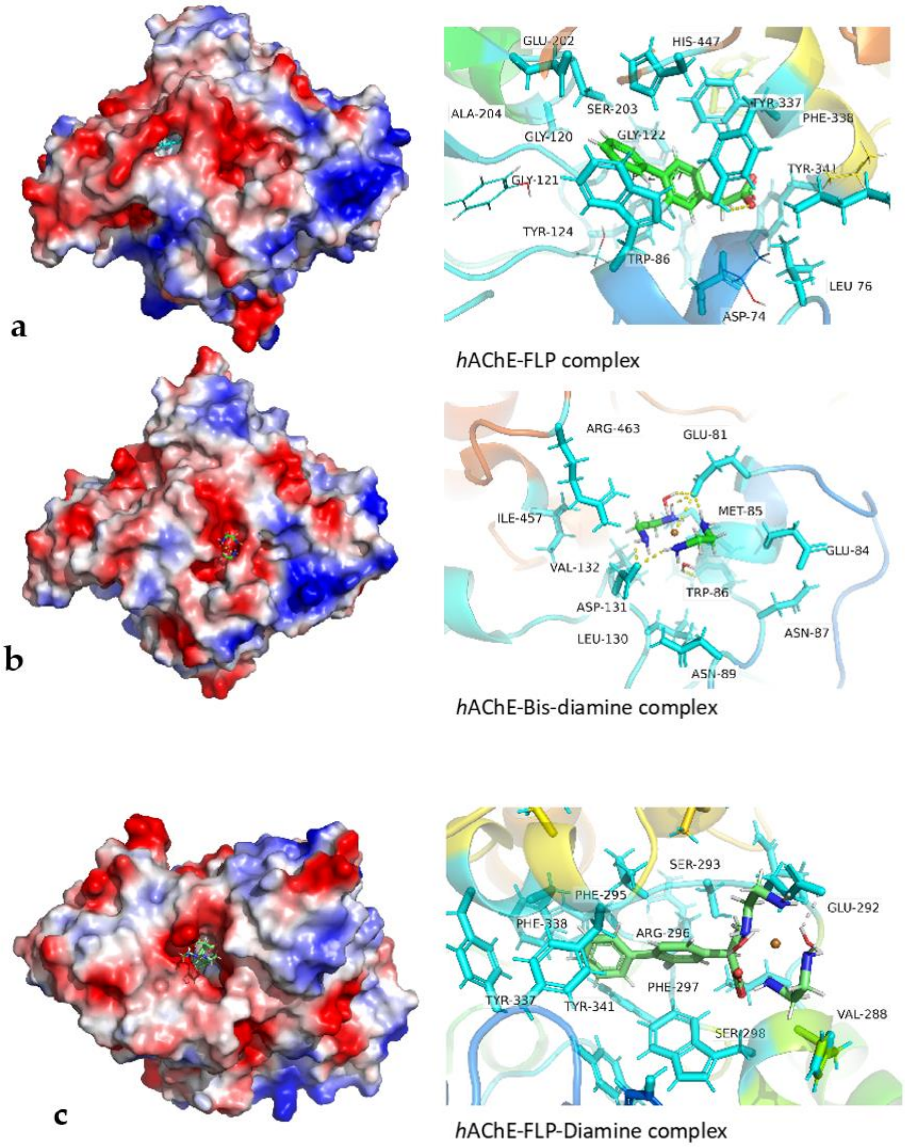

Figure 3. Binding mode of flurbiprofen (FLP) (**a**), bis-diamine metal complex (**b**), FLP-bis-diamine metal complex (**c**) in the catalytic and peripheral pocket of *h*AChE. The figures on the left show electrostatic potential surface (generated with PyMol) and ligand binding cavities (gorge).

The FLP-bis-diamine complex reached the entrance at the gorge of CAS while interacting with Tyr^{341}. Non-polar interactions to Tyr^{337}, Phe^{338} and Phe^{295} in the CAS gorge stabilize the complex interactions within the active site (Figure 3c). The complex cannot enter entirely into the CAS gorge; it also loses the interactions with Trp^{286}. The bis-diamine metal complex interacts with Glu^{392} viz bound water molecule. The interactions within the CAS gorge account for high binding energy and stabilized ligand binding. The Phe^{295} interactions, seen here, are also responsible for donepezil inhibition towards *h*AChE [35,37]. Zephycandidine A and galanthamine have been shown to interact with AChE via Tyr^{337} and Trp^{286}.

In the case of *h*BChE, the bis-diamine metal complex shows backbone interactions with Gln^{119}, Ser^{287}, Leu^{286} and Val^{288} (Figure 4b). The metal complex is stabilized by Gly^{116}, Gly^{117}, Gln^{119}, Phe^{329} and Tyr^{332}. FLP interacts with *h*BChE via π–π stacking to Trp^{82} and Phe^{329}, while Asp^{70}, Ser^{79}, Gly^{115}, Gly^{116}, Ser^{198}, Ala^{328}, Tyr^{332}, Trp^{430} and His^{438} stabilize the ligand binding (Figure 4a). Here it seems that a highly electronegative fluorine atom in FLP was the reason for its strong interactions with Gly^{115} and Gly^{116}. Tarcine, an

inhibitor of *h*BChE, has also been found to share the same binding site [38] and its binding is stabilized by π–π stacking with Trp^{82}.

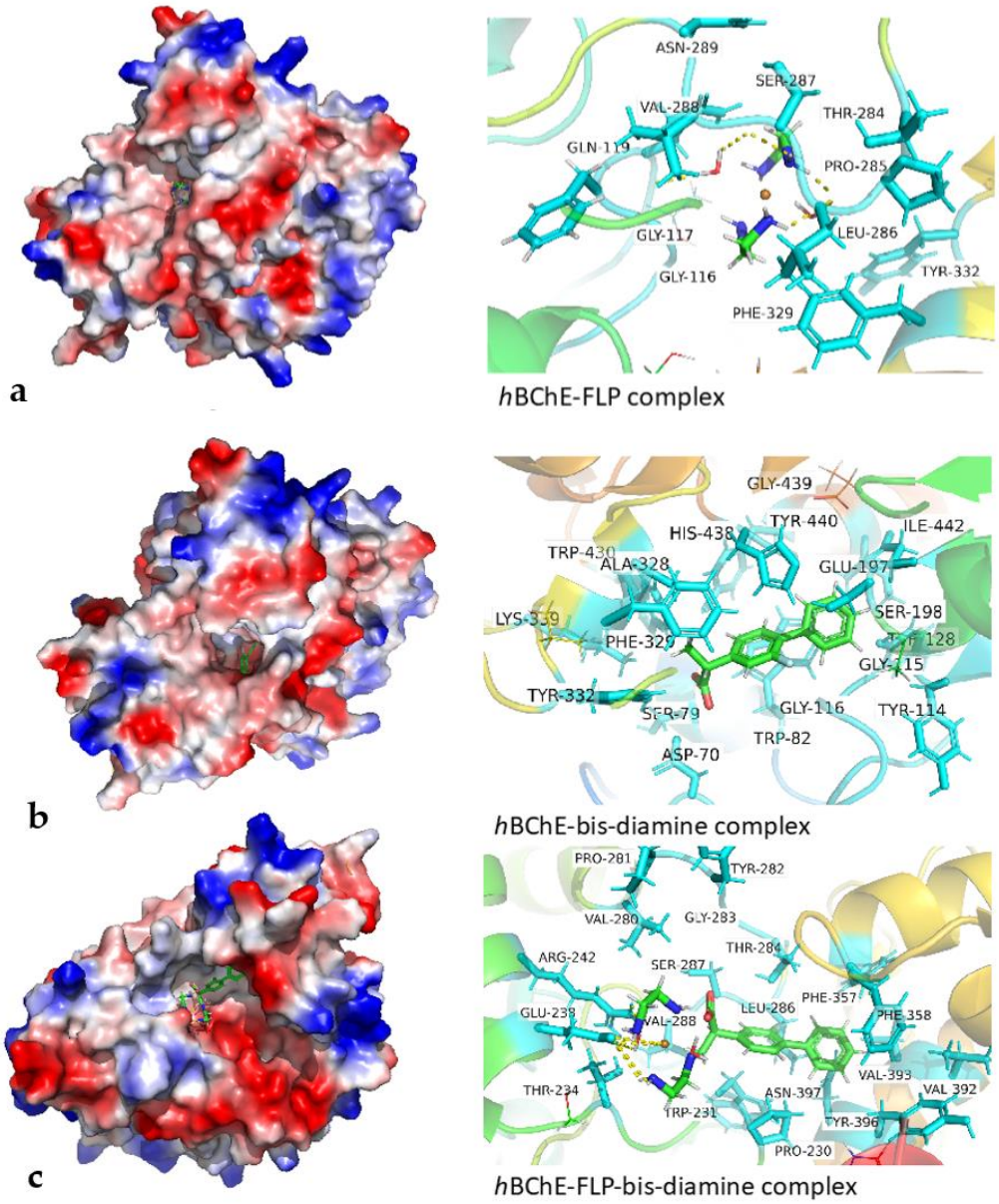

Figure 4. Binding mode of FLP (**a**), bis-diamine metal complex (**b**), FLP-bis-diamine metal complex (**c**) in the catalytic and peripheral pocket of *h*BChE. The figures on the left show electrostatic potential surface (generated with PyMol) and ligand binding cavities (gorge).

The FLP-bis-diamine complex was found to perfectly occupy the position in the *h*BChE PAS and CAS gorge. The metal ion was found to coordinate with Glu^{238}. Here, interactions with *h*BChE show that FLP-bis-diamine complex enters the gorge fully, where Phe^{357}, Phe^{358} and Tyr^{396} are involved in π–π stacking. While FLP loses the π–π stacking to Trp^{82}, its binding is stabilized by Leu^{286}, Val^{293} and Asn^{396} (Figure 4c). The results suggest that the FLP-bis-diamine complex may be an ideal *h*AChE and *h*BuChE inhibitor due to the presence of extensive π–π stacking and hydrogen and hydrophobic interactions. The metal-bound FLP-bis-diamine complex shows stable interactions in comparison to individual the FLP or bis-diamine metal complex.

4. Conclusions

Since no proper cure for AD exists, cholinesterase inhibitors such as Donepezil have delayed the progression of AD therapeutically. Second-generation cholinesterase inhibitors, such as rivastigmine and galantamine, have entered the treatment of AD. This study aims to develop novel inhibitors to further advance AD treatment by utilizing the fascinating properties of transition metal complexes [39–41]. We have synthesized and characterized Zn(II) and Cu(II) transition metal complexes with flurbiprofen and diamines. All the metal complexes demonstrated distorted octahedral geometry on the basis of electronic spectra and B.M values. Metal complexes, along with 1,2-diaminoethane, 1,3-diaminopropane, and flurbiprofen, show an electrolytic nature, while simple metal flurbiprofen complexes are non-electrolytic. Among all synthesized metal complexes, most of the synthesized metal complexes exhibited elevated cholinesterase inhibitory activity. Copper complexes exhibit the highest activity against the cholinesterase enzyme as compared to zinc metal complexes. Furthermore, bis (1,2-diaminoethane) metal flurbiprofen complexes and bis (1,3-diaminopropane) metal flurbiprofen complexes show better cholinesterase inhibition as compared to simple metal flurbiprofen complexes. In conclusion, the diamines synthesized in this study show potential in AD treatment as novel cholinesterase inhibitors.

Supplementary Materials: The following are available online at https://www.mdpi.com/2073-4352/11/2/208/s1, Figure S1: ORTEP diagram of 2b with thermal ellipsoids drawn at 100% probability level. The H-atoms are shown as small circles of arbitrary radii. Symmetry code i = 1 − x, − y, 1 − z, Table S1: UV/VIS, IR and Molar conductivities of the metal complexes, Table S2: Elemental analysis and magnetic susceptibility data of the complexes, Table S3: Bond lengths [Å] and angles [°] for 2b.

Author Contributions: Conceptualization, C.L. and M.I.T.; methodology, M.J., W.X.Z. and R.A.; software, M.F.u.R.; validation, M.J. and N.S. and F.K.; formal analysis, W.X.Z.; investigation, M.I.T., M.J., H.E., and F.K.; data curation, M.F.u.R.; writing—original draft preparation, C.L, M.J., M.B. and F.K.; writing—review and editing, M.F.u.R., M.J., and F.K.; visualization, W.X.Z.; supervision, W.X.Z.; project administration, W.X.Z., C.L.; funding acquisition, C.L. and M.I.T. All authors have read and agreed to the published version of the manuscript.

Funding: Funding in the Lu lab was provided by the Fundamental Research Funds for the Central Universities (2232021G-04), Shanghai Science and Technology Committee (19ZR1471100), the National College Student Innovation Experiment Program (105-03-0178028, 105-03-0178029, 105-03-0178229, 105-03-0178139).

Conflicts of Interest: The authors declare no conflict of interest.

References

1. Bakkour, A.; Morris, J.C.; Dickerson, B.C. The cortical signature of prodromal AD: Regional thinning predicts mild AD dementia. *Neurology* **2009**, *72*, 1048–1055. [CrossRef]
2. Liu, Y.; Patricelli, M.P.; Cravatt, B.F. Activity-based protein profiling: The serine hydrolases. *Proc. Natl. Acad. Sci. USA* **1999**, *96*, 14694–14699. [CrossRef]
3. Simon, G.M.; Cravatt, B.F. Activity-based proteomics of enzyme superfamilies: Serine hydrolases as a case study. *J. Biol. Chem.* **2010**, *285*, 11051–11055. [CrossRef]
4. Rosenbek, J.C.; Troche, M.S. Progressive neurologic disease and dysphagia (including Parkinson's disease, multiple sclerosis, amyotrophic lateral sclerosis, myasthenia gravis, post-polio syndrome). In *Principles of Deglutition*; Springer: Berlin/Heidelberg, Germany, 2013; pp. 395–409.
5. Withiam-Leitch, S.; Pullicino, P. Ataxic hemiparesis with bilateral leg ataxia from pontine infarct. *J. Neurol. Neurosurg. Psychiatry* **1995**, *59*, 557. [CrossRef]
6. Shaw, K.; Aracava, Y.; Akaike, A.; Daly, J.; Rickett, D.; Albuquerque, E. The reversible cholinesterase inhibitor physostigmine has channel-blocking and agonist effects on the acetylcholine receptor-ion channel complex. *Mol. Pharmacol.* **1985**, *28*, 527–538. [PubMed]
7. Gallucci, M.; Spagnolo, P.; Aricò, M.; Grossi, E. Predictors of response to cholinesterase inhibitors treatment of Alzheimer's disease: Date mining from the TREDEM registry. *J. Alzheimer's Dis.* **2016**, *50*, 969–979. [CrossRef] [PubMed]
8. Burns, A.; Rossor, M.; Hecker, J.; Gauthier, S.; Petit, H.; Möller, H.-J.; Rogers, S.; Friedhoff, L. The Effects of Donepezil in Alzheimer's Disease–Results from a Multinational Trial1. *Dement. Geriatr. Cogn. Disord.* **1999**, *10*, 237–244. [CrossRef] [PubMed]
9. Birks, J.S.; Evans, J.G. Rivastigmine for Alzheimer's disease. *Cochrane Database Syst. Rev.* **2015**. [CrossRef]

10. Loy, C.; Schneider, L. Galantamine for Alzheimer's disease and mild cognitive impairment. *Cochrane Database Syst. Rev.* **2006**. [CrossRef] [PubMed]
11. Morris, J.C.; Cyrus, P.A.; Orazem, J.; Mas, J.; Bieber, F.; Ruzicka, B.B.; Gulanski, B. Metrifonate benefits cognitive, behavioral, and global function in patients with Alzheimer's disease. *Neurology* **1998**, *50*, 1222–1230. [CrossRef]
12. Mehta, M.; Adem, A.; Sabbagh, M. New acetylcholinesterase inhibitors for Alzheimer's disease. *Int. J. Alzheimer's Dis.* **2012**, *2012*. [CrossRef] [PubMed]
13. Tang, X.C.; De Sarno, P.; Sugaya, K.; Giacobini, E. Effect of huperzine A, a new cholinesterase inhibitor, on the central cholinergic system of the rat. *J. Neurosci. Res.* **1989**, *24*, 276–285. [CrossRef] [PubMed]
14. Young, S.; Fabio, K.; Guillon, C.; Mohanta, P.; Halton, T.A.; Heck, D.E.; Flowers II, R.A.; Laskin, J.D.; Heindel, N.D. Peripheral site acetylcholinesterase inhibitors targeting both inflammation and cholinergic dysfunction. *Bioorganic Med. Chem. Lett.* **2010**, *20*, 2987–2990. [CrossRef] [PubMed]
15. Chang, Y.-C.; Wang, J.D.; Hahn, R.A.; Gordon, M.K.; Joseph, L.B.; Heck, D.E.; Heindel, N.D.; Young, S.C.; Sinko, P.J.; Casillas, R.P. Therapeutic potential of a non-steroidal bifunctional anti-inflammatory and anti-cholinergic agent against skin injury induced by sulfur mustard. *Toxicol. Appl. Pharmacol.* **2014**, *280*, 236–244. [CrossRef] [PubMed]
16. Young, S.C.; Fabio, K.M.; Huang, M.T.; Saxena, J.; Harman, M.P.; Guillon, C.D.; Vetrano, A.M.; Heck, D.E.; Flowers, R.A.; Heindel, N.D. Investigation of anticholinergic and non-steroidal anti-inflammatory prodrugs which reduce chemically induced skin inflammation. *J. Appl. Toxicol.* **2012**, *32*, 135–141. [CrossRef]
17. Jamil, M.; Sultana, N.; Ashraf, R.; Sarfraz, M.; Tariq, M.I.; Mustaqeem, M. Tris-diamine-derived transition metal complexes of flurbiprofen as cholinesterase inhibitors. *Trop. J. Pharm. Res.* **2018**, *17*, 451–459. [CrossRef]
18. Colovic, M.B.; Krstic, D.Z.; Lazarevic-Pasti, T.D.; Bondzic, A.M.; Vasic, V.M. Acetylcholinesterase inhibitors: Pharmacology and toxicology. *Curr. Neuropharmacol.* **2013**, *11*, 315–335. [CrossRef]
19. Louie, A.Y.; Meade, T.J. Metal complexes as enzyme inhibitors. *Chem. Rev.* **1999**, *99*, 2711–2734. [CrossRef]
20. Eremina, J.A.; Lider, E.V.; Samsonenko, D.G.; Sheludyakova, L.A.; Berezin, A.S.; Klyushova, L.S.; Ostrovskii, V.A.; Trifonov, R.E. Mixed-ligand copper (II) complexes with tetrazole derivatives and 2, 2′-bipyridine, 1, 10-phenanthroline: Synthesis, structure and cytotoxic activity. *Inorg. Chim. Acta* **2019**, *487*, 138–144. [CrossRef]
21. Matesanz, A.I.; Caballero, A.B.; Lorenzo, C.; Espargaró, A.; Sabaté, R.; Quiroga, A.N.G.; Gamez, P. Thiosemicarbazone Derivatives as Inhibitors of Amyloid-β Aggregation: Effect of Metal Coordination. *Inorg. Chem.* **2020**, *59*, 6978. [CrossRef]
22. Gomes, L.M.; Vieira, R.P.; Jones, M.R.; Wang, M.C.; Dyrager, C.; Souza-Fagundes, E.M.; Da Silva, J.G.; Storr, T.; Beraldo, H. 8-Hydroxyquinoline Schiff-base compounds as antioxidants and modulators of copper-mediated Aβ peptide aggregation. *J. Inorg. Biochem.* **2014**, *139*, 106–116. [CrossRef]
23. Deraeve, C.; Pitié, M.; Mazarguil, H.; Meunier, B. Bis-8-hydroxyquinoline ligands as potential anti-Alzheimer agents. *New J. Chem.* **2007**, *31*, 193–195. [CrossRef]
24. Ellman, J.; Mendel, D.; Anthony-Cahill, S.; Noren, C.J.; Schultz, P.G. Biosynthetic method for introducing unnatural amino acids site-specifically into proteins. *Methods Enzymol.* **1991**, *202*, 301–336. [PubMed]
25. Santini, C.; Pellei, M.; Gandin, V.; Porchia, M.; Tisato, F.; Marzano, C. Advances in Copper Complexes as Anticancer Agents. *Chem. Rev.* **2014**, *114*, 815–862. [CrossRef] [PubMed]
26. Figiel, P.J.; Kirillov, A.M.; Guedes da Silva, M.F.C.; Lasri, J.; Pombeiro, A.J.L. Self-assembled dicopper(ii) diethanolaminate cores for mild aerobic and peroxidative oxidation of alcohols. *Dalton Trans.* **2010**, *39*, 9879–9888. [CrossRef] [PubMed]
27. Dias, S.S.P.; Kirillova, M.V.; André, V.; Kłak, J.; Kirillov, A.M. New tricopper(ii) cores self-assembled from aminoalcohol biobuffers and homophthalic acid: Synthesis, structural and topological features, magnetic properties and mild catalytic oxidation of cyclic and linear C5–C8 alkanes. *Inorg. Chem. Front.* **2015**, *2*, 525–537. [CrossRef]
28. Eckert, P.K.; Vieira, I.d.S.; Gessner, V.H.; Börner, J.; Strohmann, C.; Herres-Pawlis, S. Simple is best: Diamine zinc complexes as unexpected catalysts in lactide polymerisation. *Polyhedron* **2013**, *49*, 151–157. [CrossRef]
29. Girek, M.; Szymański, P. Tacrine hybrids as multi-target-directed ligands in Alzheimer's disease: Influence of chemical structures on biological activities. *Chem. Pap.* **2019**, *73*, 269–289. [CrossRef]
30. Jamil, M.; Sultana, N.; Sarfraz, M.; Tahir, M.N.; Tariq, M.I. Diamines Derived Transition Metal Complexes of Naproxen: Synthesis, Characterization and Urease Inhibition Studies. *Iran. J. Chem. Chem. Eng. (Ijcce)* **2020**, *39*, 45–57. [CrossRef]
31. Krieger, E.; Vriend, G. YASARA View—Molecular graphics for all devices—From smartphones to workstations. *Bioinformatics* **2014**, *30*, 2981–2982. [CrossRef]
32. Bilal, S.; Mudassir Hassan, M.; Fayyaz ur Rehman, M.; Nasir, M.; Jamil Sami, A.; Hayat, A. An insect acetylcholinesterase biosensor utilizing WO3/g-C3N4 nanocomposite modified pencil graphite electrode for phosmet detection in stored grains. *Food Chem.* **2021**, *346*, 128894. [CrossRef] [PubMed]
33. Ellman, G.L.; Courtney, K.D.; Andres Jr, V.; Featherstone, R.M. A new and rapid colorimetric determination of acetylcholinesterase activity. *Biochem. Pharmacol.* **1961**, *7*, 88–95. [CrossRef]
34. Sami, A.J.; Bilal, S.; Khalid, M.; Shakoori, F.R.; Shakoori, A. Effect of crude neem (Azadirachta indica) powder and azadirachtin on the growth and acetylcholinesterase activity of Tribolium castaneum (Herbst) (Coleoptera: Tenebrionidae). *Pak. J. Zool* **2016**, *48*, 881–886.
35. Kryger, G.; Silman, I.; Sussman, J.L. Structure of acetylcholinesterase complexed with E2020 (Aricept®): Implications for the design of new anti-Alzheimer drugs. *Structure* **1999**, *7*, 297–307. [CrossRef]

36. Bai, F.; Xu, Y.; Chen, J.; Liu, Q.; Gu, J.; Wang, X.; Ma, J.; Li, H.; Onuchic, J.N.; Jiang, H. Free energy landscape for the binding process of Huperzine A to acetylcholinesterase. *Proc. Natl. Acad. Sci. USA* **2013**, *110*, 4273–4278. [CrossRef] [PubMed]
37. Berg, L.; Andersson, C.D.; Artursson, E.; Hörnberg, A.; Tunemalm, A.-K.; Linusson, A.; Ekström, F. Targeting acetylcholinesterase: Identification of chemical leads by high throughput screening, structure determination and molecular modeling. *PLoS ONE* **2011**, *6*, e26039. [CrossRef] [PubMed]
38. Tripathi, R.K.; Sasi, M.V.; Gupta, S.K.; Krishnamurthy, S.; Ayyannan, S.R. Design, synthesis, and pharmacological evaluation of 2-amino-5-nitrothiazole derived semicarbazones as dual inhibitors of monoamine oxidase and cholinesterase: Effect of the size of aryl binding site. *J. Enzym. Inhib. Med. Chem.* **2018**, *33*, 37–57. [CrossRef] [PubMed]
39. Renfrew, A.K. Transition metal complexes with bioactive ligands: Mechanisms for selective ligand release and applications for drug delivery. *Metallomics* **2014**, *6*, 1324–1335. [CrossRef] [PubMed]
40. Jaros, S.W.; Guedes da Silva, M.F.C.; Florek, M.; Smoleński, P.; Pombeiro, A.J.L.; Kirillov, A.M. Silver(I) 1,3,5-Triaza-7-phosphaadamantane Coordination Polymers Driven by Substituted Glutarate and Malonate Building Blocks: Self-Assembly Synthesis, Structural Features, and Antimicrobial Properties. *Inorg. Chem.* **2016**, *55*, 5886–5894. [CrossRef] [PubMed]
41. Dabrowiak, J.C. *Metals in Medicine*; John Wiley & Sons: Hoboken, NJ, USA, 2017.